Nuclear Inst. and Methods in Physics Research, A 886 (2018) 55–60

Contents lists available at ScienceDirect

Nuclear Inst. and Methods in Physics Research, A

journal homepage: www.elsevier.com/locate/nima

Characterization of a ^{6}Li enriched Cs_2LiYCl_6:Ce scintillator and its application as a γ-ray detector

Jianguo Qin [a,b], Caifeng Lai [a], Xinxin Lu [a], Pu Zheng [a,*], Tonghua Zhu [a], Rong Liu [a], Bangjiao Ye [b], Xinwei Zhang [c]

[a] Institute of Nuclear Physics and Chemistry, China Academy of Engineering Physics, P.O. Box 213, Mianyang 621900, China
[b] Department of Modern Physics, University of Science and Technology of China, Hefei 230026, China
[c] Institute of Applied Physics and Computational Mathematics, P.O. Box 8009, Beijing 100088, China

ARTICLE INFO

Keywords:
Cs_2LiYCl_6:Ce detector
γ-ray response functions
Detection efficiency
Pulse shape discrimination

ABSTRACT

In this work, we characterize the γ-ray response and efficiency for a cylindrical inorganic Cs_2LiYCl_6:Ce detector 1″ in diameter and 1″ in height. The energy resolution and linearity are obtained from 21 γ-rays with energies ranging from 0.026 to 2.447 MeV. In addition, the neutron γ-ray discrimination is validated by measuring a ^{252}Cf radioisotope. Gamma-ray response functions and matrix below 7 MeV are simulated using a Monte Carlo approach and validated through the unfolded γ-ray spectra.

1. Introduction

NaI:Tl and HPGe are the most widely used γ-ray detectors in γ-ray dosimetry or spectroscopy. HPGe is appropriate for accurately measuring γ-rays with high detection efficiency and excellent energy resolution. However, these photon spectrometers are limited for use in mixed neutron/γ-ray (n/γ) fields, as the neutron response cannot be corrected. In addition, neutron damage is a serious issue for HPGe detectors and they require very low working temperatures [1].

Some scintillation detectors are preferable to HPGe semiconductors, because they can be operated at room temperature and can discriminate γ-rays from neutrons in mixed n/γ fields. Recently, researchers have developed novel scintillators for neutron and γ radiation detection [2,3]; one such scintillator is the elpasolite crystal, Cs_2LiYCl_6:Ce(CLYC) [4–6]. Due to the presence of ^{6}Li and ^{35}Cl in the crystal, CLYC can be used for both thermal and fast neutrons utilizing two separate kinds of nuclear reactions ^{6}Li(n,α), ^{35}Cl(n,p)^{35}S and ^{35}Cl(n, α)^{35}S [7,8], and it can also be used as a substitute for Lithium glass to measure both thermal neutrons and fast neutrons [9–11]. Furthermore, Due to the high light output of CLYC to gamma rays (approximately 20,000 photons/MeV) and the excellent proportionality, the energy resolution for 662 keV gamma rays can reach 4% (full width at half-maximum) [12]. It can be used as a γ-spectrometry with good performance. In addition, its excellent n/γ discrimination enables CLYC especially attractive for using in n/γ mixed fields and for a variety of nuclear safeguard applications where ^{3}He tube replacement is required [13,14].

In order to measure the γ-ray spectrum accurately, γ-ray detector response functions must be validated through experiment and Monte Carlo (MC) simulations. The neutron response should be removed within an n/γ mixed field. The experiments are conducted using several γ sources with energies ranging between 0.026 and 2.447 MeV, and the n/γ mixed fields is emitted by a 0.27 μCi ^{252}Cf neutron source. The crystal response function simulation utilizes Monte-Carlo N-Particle (MCNP) code. In this paper, we present the experimental and simulated results to determine the response functions for a 1″ × 1″ ^{6}Li enriched CLYC scintillator detector.

2. Experiment and simulation details

2.1. CLYC detector and theory

The elpasolite crystal used in this work ($Cs_2^{6}LiYCl_6$:Ce, 95% ^{6}Li enriched isotope and doped with 0.5 mol% Ce^{3+}) has a 3.31 g/cm^3 density and Φ1″ × 1″ dimensions; it was grown by Radiation Monitoring Devices Inc. (RMD) [15]. The thickness the crystal encapsulation entrance window is 0.5 mm. A picture of the CLYC detector is shown in Fig. 1(a). The crystal is mounted on a Hamamatsu R6231-100 (PMT) with 2″ diameter and integrated with a Hamamatsu E1198-26 voltage divider. High voltage for the PMT is –1400 V.

The crystal has three light decay constants due to different light emission from neutrons passing through the crystal medium [9,16]. The

* Corresponding author.
E-mail address: zhengpu@aliyun.com (P. Zheng).

https://doi.org/10.1016/j.nima.2017.11.053
Received 27 March 2017; Received in revised form 8 November 2017; Accepted 16 November 2017
Available online 4 January 2018
0168-9002/

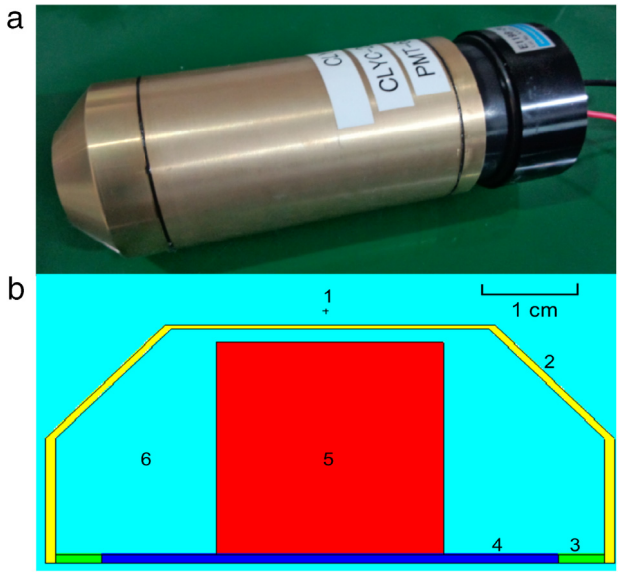

Fig. 1. CLYC detector photo and simulation schematic: 1-Radioactive source, 2-Aluminum housing, 3-Organic glass bracket, 4-PMT face, 5-CLYC crystal, and 6. Air. (a) Detector photo, a 1″ (diameter) × 1″ (height) crystal has been mounted on a 2″ (diameter) × 10 cm (length) PMT, (b) CLYC detector simulation schematic.

sensitivity to thermal neutron is given by the ^{6}Li (n, ^{3}He)T reaction; note that an alpha particle along with a tritium nuclei is emitted. The deposited energy from the reaction products creates scintillations. Consequently, a signal is formed at the detection system output. The Q-value for this reaction is 4.782 MeV. Furthermore, the ^{7}Li isotope has two neutron reactions, as shown in formula (2) and (3). The other two important nuclear reactions are shown in formula (4) and (5). The neutron cross sections in the energy region ranging from 1.4 to 10 MeV are large enough to use for fast neutron detection.

$$\mathrm{n} + {}^{6}_{3}\mathrm{Li} \rightarrow \mathrm{T} + {}^{4}_{2}\mathrm{He} + 4.782\ \mathrm{MeV} \quad (1)$$

$$\mathrm{n} + {}^{7}_{3}\mathrm{Li} \rightarrow \mathrm{T} + {}^{4}_{2}\mathrm{He} + \mathrm{n}' - 2.467\ \mathrm{MeV} \quad (2)$$

$$\mathrm{n} + {}^{7}_{3}\mathrm{Li} \rightarrow {}^{6}_{3}\mathrm{Li} + 2\mathrm{n}' - 7.249\ \mathrm{MeV} \quad (3)$$

$$\mathrm{n} + {}^{35}_{17}\mathrm{Cl} \rightarrow {}^{35}_{16}\mathrm{S} + \mathrm{p} + 0.614\ \mathrm{MeV} \quad (4)$$

$$\mathrm{n} + {}^{35}_{17}\mathrm{Cl} \rightarrow {}^{32}_{15}\mathrm{P} + \alpha + 0.943\ \mathrm{MeV} \quad (5)$$

The interactions between the impinging γ-rays and the crystal are mainly photoelectric absorption, Compton scattering, and pair production (when $E_\gamma > 1.022$ MeV). The main emission is due to Ce^{3+}/STE (self-trapped excitons), the secondary emission is Core-to-Valence Luminescence (CVL) and decays very quickly. If the crystal is large enough, this light will be absorbed by the Ce^{3+} ions and re-emitted at a slower rate than CVL. This feature is absent in the output pulse produced by a neutron irradiation event. Thus, n/γ discrimination is possible via pulse shape discrimination (PSD).

2.2. Experimental setup and irradiation

For γ-ray experiments, the CLYC detector is irradiated using several standard gamma sources with energies ranging from 0.026 to 2.447 MeV. Details for these gamma sources are shown in Table 1. The output from the PMT is delivered directly into a DT5751 CAEN digitizer and controlled using LabVIEW software for further data processing; a block diagram of the electronic circuit is shown in Fig. 2. For neutron experiments, the CLYC detector was irradiated with a ^{252}Cf source. The neutron intensity for ^{252}Cf radioisotope is about 10^4 s^{-1}.

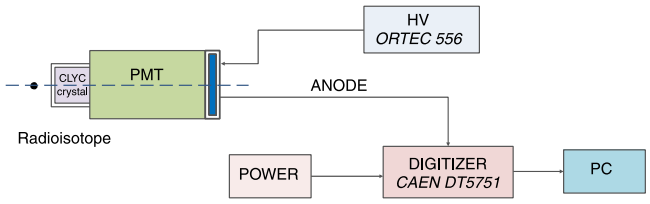

Fig. 2. The detector and block diagram for the electronic circuit.

2.3. Simulation details

The scintillator and γ-ray radioactive sources have been modeled in MCNP5. A schematic view of the simulation model is shown in Fig. 1(b). The response function is obtained using the "F8" tally, which provides pulse height distribution in the CLYC scintillator sensitive volume based on the ENDF/BVII.1 library [17]. The "FT8 GEB" card is used to consider the detector resolution, with parameters coming from experimental measurements. To validate the simulation, the response function calculation for a standard point gamma-ray sources is calculated; the distance between the point source and the CLYC detector front surface is 2 mm, which is the same as in the experiment. Additionally, the response matrix for a parallel γ-ray beam is also determined and used in spectra unfolding.

3. Results

3.1. CLYC detector characteristics

3.1.1. Linearity and energy resolution

Measurements were carried out at the Institute of Nuclear Physics and Chemistry (INPC), China Academy of Engineering Physics (CAEP). First, the γ-ray and neutron responses were measured with 21 γ-rays as shown in Fig. 3(a). The most maximum value of standard errors for the calculated energy points is less than 0.86%. The CLYC detector exhibited excellent linearity, with an adjusted R-Square value of 0.9999 for the experimental data.

Scintillators have intrinsic non-proportionality response (nPR) between scintillator light yield and photon deposition which affects their energy resolution. The nPR can be explained as that it originates from the non-linear interactions of electrons and holes in a tiny excitation volume leading to a quenching of luminescence [18]. Gamma-ray non-proportionality can be traced back experimentally. Following the ideas of Pieter Dorenbos [19] and Wahyu Setyawan et al. [20], the degree of photon nPR can be quantified [21]. The nPR normalized to 662 keV is show in Fig. 3(b), the maximum nPR is less than 1.22%.

Energy resolutions for γ-rays were obtained by fitting the experiment data for standard γ-ray sources using the Gaussian function $f(x) = k_0 + \frac{A}{\sigma\sqrt{2\pi}} e^{-\frac{1}{2}(\frac{x-\mu}{\sigma})^2}$, and the parameter σ is related to the full width at half maximum (FWHM) of the peak according to FWHM $= 2\sqrt{2\ln 2}\sigma$. Furthermore, the FWHM is described as Eq. (5) in the MCNP simulation code [22] and shown in Fig. 4(a). The parameters a, b, and c can be obtained according to fitting the FWHMs and will be used to calculate the γ-ray response with energy resolution. Moreover, the energy resolution can also be represented by a percentage ratio (FWHM/E_γ) × 100%, as shown in Fig. 4(b). The energy resolution is 4.48% at 662 keV, which is better than the commonly used NaI:Tl crystal [23].

$$\mathrm{FWHM} = a + b\sqrt{E + cE^2} \quad (6)$$

Table 1
Parameters for the γ-ray radioactive sources.[1]

Radioactive sources	Activity (kBq)	Energy (MeV)	Intensity (%)	Radiation type
^{241}Am	40.9	0.026	2.4	γ-rays
		0.059	35.9	
^{137}Cs	31.3	0.032	5.53	X-ray (^{137}Ba-K_α)
		0.037	1.32	X-ray (^{137}Ba-K_β)
		0.662	85	γ-ray
^{60}Co	7.3	1.173	0.9985	γ-rays
		1.332	0.9998	
^{133}Ba	17.3	0.081	0.3668	γ-rays
		0.356	0.799	
^{152}Eu	19.4	0.122	0.2858	γ-rays
		0.245	0.0758	
		0.344	0.265	
		0.779	0.1294	
		1.408	0.21	
^{226}Ra	30.2	0.186	0.0351	γ-rays
		0.295	0.1815	
		0.352	0.351	
		0.609	0.446	
		1.120	0.147	
		2.204	0.0498	
		2.447	0.0155	

[1] All the parameters are recommended nuclear decay data from *AEA TECHNOLOGY*.

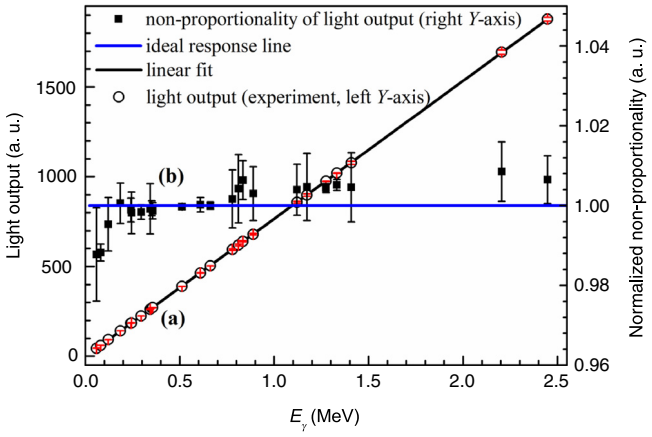

Fig. 3. Light output and nPR for the CLYC detector using standard gamma ray point sources.

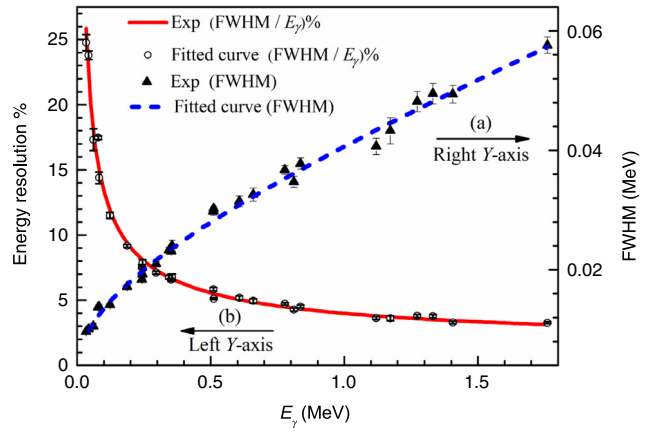

Fig. 4. Energy resolution for γ-rays measured using the CLYC detector. The right and the left axis represent the (a) energy and the (b) percentage ratio, respectively.

3.1.2. Neutron γ-ray discrimination

The pulse shape and height are two important parameters that are used to describe neutron and γ-ray resolutions. The gamma equivalent energy (GEE) for a full energy thermal neutron peak is above 3 MeV.

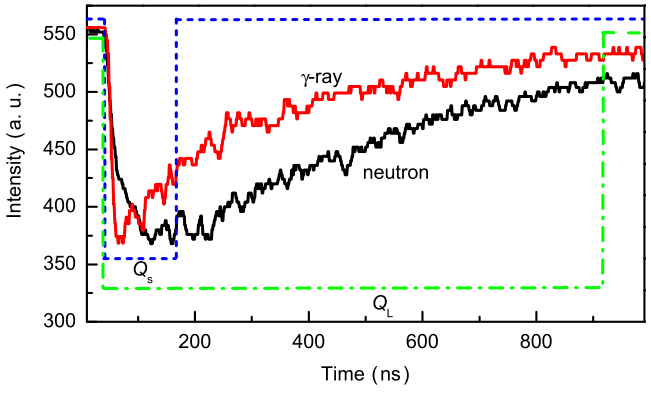

Fig. 5. Temporal detector response (CLYC + PMT) to neutron (black) and γ-ray (red) radiation.

Such a high GEE value provides a good basis for pulse height discrimination (PHD); as a result PHD is effective for many scenarios where only lower-energy γ-rays are observed. On the other hand, better PSD detection can be achieved by examining the prominent pulse shape discrepancy. Charge integral comparison method is used in this work. Typical pulses for neutron and γ-ray irradiating the CLYC crystal are shown in Fig. 5, Q_S and Q_L represent the integral charge at different time intervals. Q_S was focused on the rising part of the trace and the fast component, $Q_L - Q_S$, was focused on the slow remainder of the trace. The PSD factors are usually described as PSD = $(Q_L - Q_S)/Q_L$. In this case the focus was on the slow tail.

A 2D n/γ discrimination plot is shown in Fig. 6. There is an excellent separation between neutrons and γ-rays. The Figure of Merit (FoM) defined as FoM = $\frac{\text{peak separation}}{\text{FWHM}_n+\text{FWHM}_\gamma}$ is 2.89 with the energy threshold 0.75 MeV. This is much better than the BC501A liquid scintillator detector [24]. Neutron events can be divided into three regions from left to right: fast neutrons (^{35}Cl), thermal neutrons (^{6}Li), and the other fast neutrons (^{35}Cl and ^{6}Li).

3.2. Gamma-ray response and detection efficiency

CLYC crystal gamma-ray response for ^{241}Am, ^{137}Cs, ^{22}Na, and ^{60}Co isotopes are shown in Fig. 7. One of the two peaks—with the energy 59.6 keV in Fig. 7(a) is a photopeak generated by γ-rays emitted from

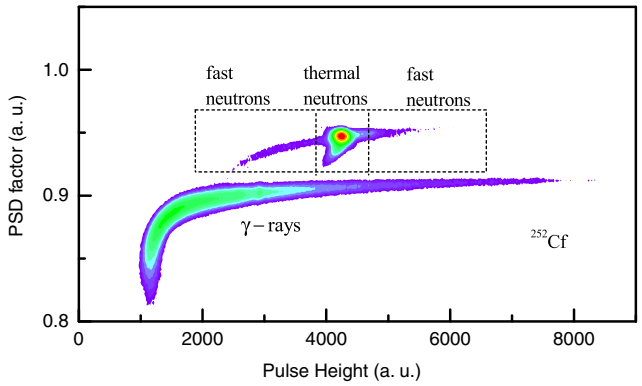

Fig. 6. PSD plot based on the collected data while irradiated by a ^{252}Cf neutron source.

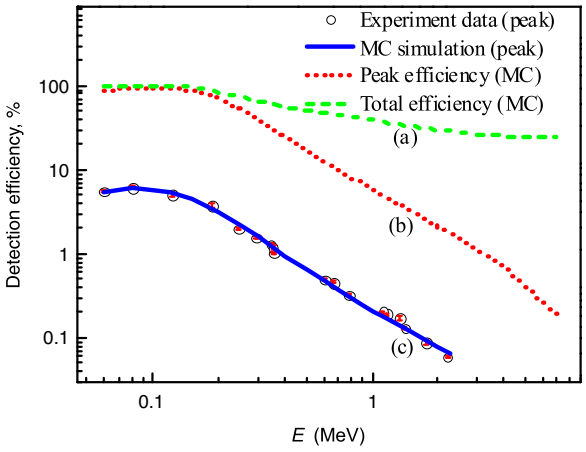

Fig. 8. CLYC detector γ-ray detection efficiency: (a) simulated total efficiency; (b) simulated photoelectric peak efficiency; (c) The blue line represents the simulated efficiency for a point γ-ray source, and the circles represent the experiment data taken at the same conditions.

the ^{241}Am isotope. The other peak is a combination of 26.3 keV and 30.7 keV [25] generated by^{241}Am γ-ray and K_α X-rays from the excited Cesium nuclei in the CLYC crystal. There are three peaks for^{137}Cs, as shown in Fig. 7(b). The three peaks from low energy to high energy are photoelectric peaks, characteristic X-ray peaks and back scattering peaks (BSP), respectively. The BSP for γ-rays of^{22}Na and^{60}Co sources are shown in Fig. 7(c) and (d). The energy of the BSP is about 200 keV, which is related to the incident gamma energy.

The measurement results in γ radiation show good agreement with the simulated pulse height distribution, except for the β particles' bremsstrahlung and the γ-ray back scattering. The two contributions are affected by experimental conditions that are not considered in the simulation. However, the result is better than R. Machrafi's [26] in the energy range $E < 0.6$ MeV.

The CLYC detector photopeak and total efficiency were simulated in MCNP as a function of energies for the parallel γ-ray beam; the results are shown in Fig. 8(a) and (b). There is little distinction between the two for $E_\gamma < 0.2$ MeV, in which photoelectric absorption is the main process. However, Compton scattering and pair production dominate as γ-ray energy increases. As a result, as the γ-ray energy increases, the discrepancy widens. In order to investigate the discrepancy between the MC simulation and the experiment, we ran another MC model with a point source placed on the central axis of the detector and 2 mm away from the detector front surface. The comparison to the experimental

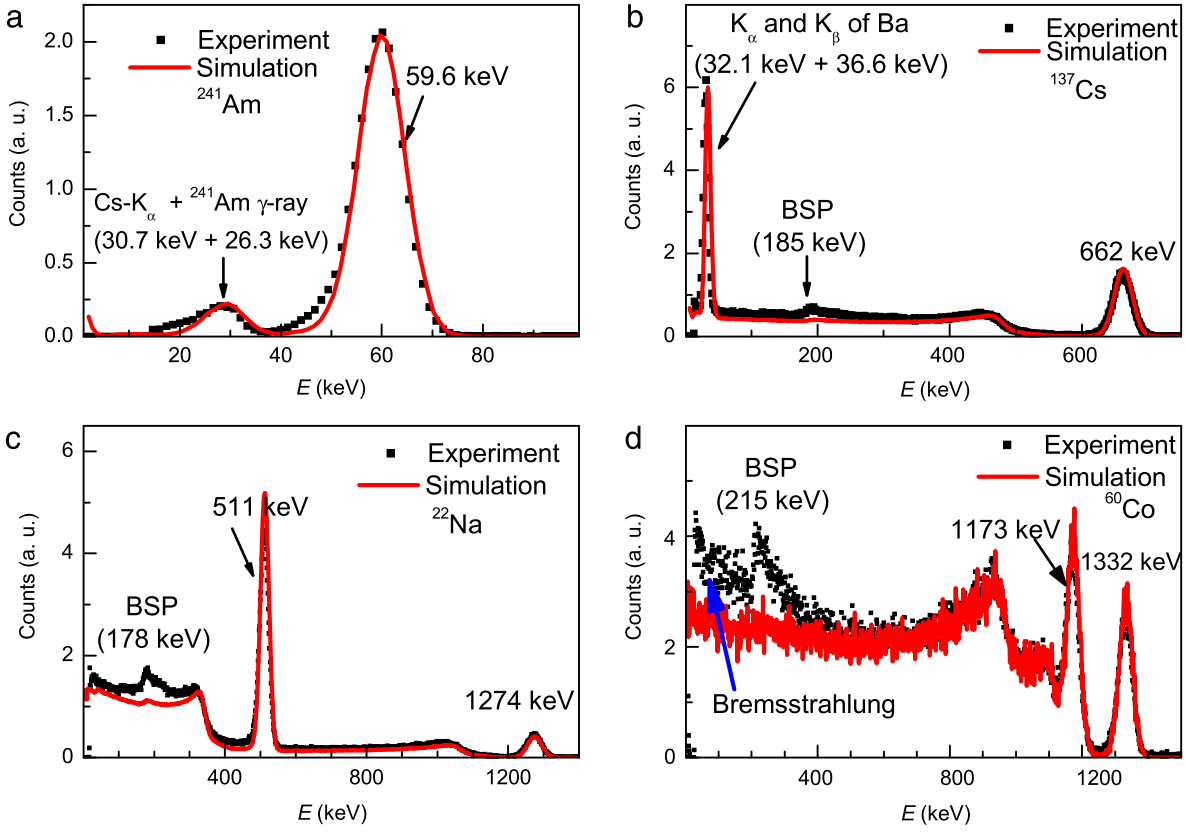

Fig. 7. γ-ray response functions from the experiment and the simulation: (a) ^{241}Am, (b) ^{137}Cs, (c) ^{22}Na, and (d) ^{60}Co.

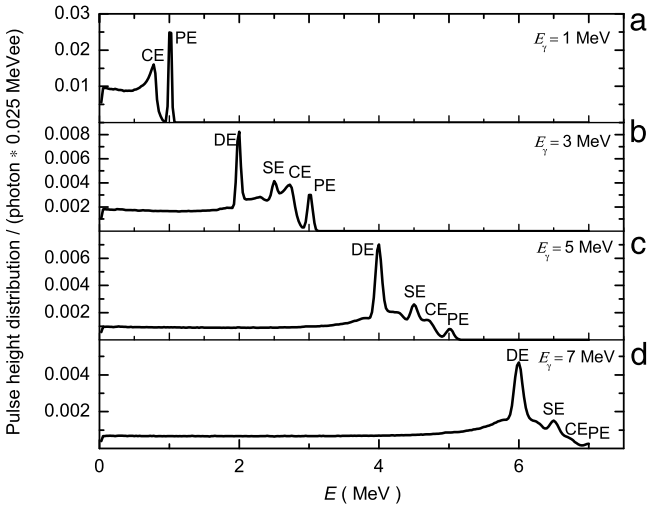

Fig. 9. Response functions for a 1″ × 1″ CLYC crystal in a parallel γ-ray beam with a 2.54 cm diameter. FE, CE, SE, and DE representing the photopeak, Compton edge, single escape peak, and double escape peak, respectively. (a) E_γ = 1 MeV, (b) E_γ = 3 MeV, (c) E_γ = 5 MeV, and (d) E_γ = 7 MeV.

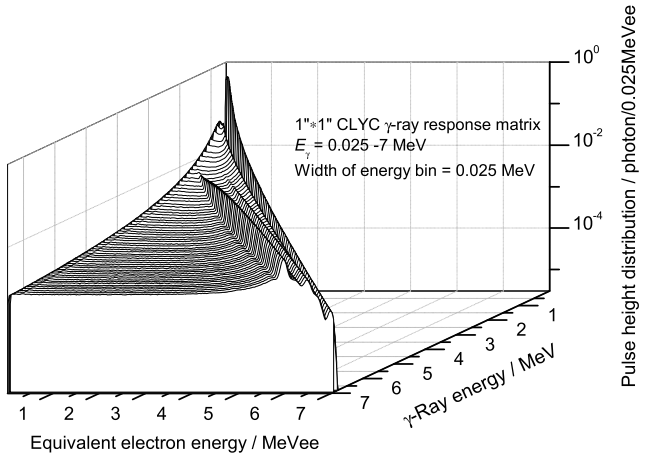

Fig. 10. Response matrix for the CLYC crystal in a parallel γ-ray beam with 2.54 cm diameter for various energies; the energy bin width is 0.025 MeV.

results for the same condition is shown in Fig. 8(c); the MC simulation results agree well with the experimental data.

3.3. γ-ray response matrix simulation

CLYC detector response functions were simulated using MCNP code, corresponding to a beam of incident γ-rays with a 2.54 cm diameter. As described above, broadening factors were used; the parameters a, b, and c described in Section 3.1 were used in the MC calculation. γ-rays response functions for 1, 3, 5, and 7 MeV are shown in Fig. 9. The results show that the three interaction processes vary with the γ-ray energies. Finally, we obtain the response 280 × 280 bins matrix for energies below 7 MeV, with a 0.025 MeV bin width. The response matrix is shown in Fig. 10, where the X, Y, and Z axes represent the recoil electron energy, the γ-rays energy, and the normalized intensity, respectively.

3.4. Validation

The CLYC detector measurement spectra were tested with γ-rays emitted by ^{60}Co, ^{152}Eu, ^{252}Cf, and ^{241}Am-Be radio sources and unfolded using the GRAVEL method [27] with the response matrix described in Section 3.3.

The measured recoiled electron spectra and the unfolded γ-ray spectra are shown in Fig. 11. From the results, we can see that the unfolded and expected γ-ray spectra agree for the standard point γ-ray sources. The γ-ray spectra measurement in a mixed neutron γ-ray fields from both the ^{252}Cf and the Am-Be source were based on charge integral method; both the measured and unfolded spectra are shown

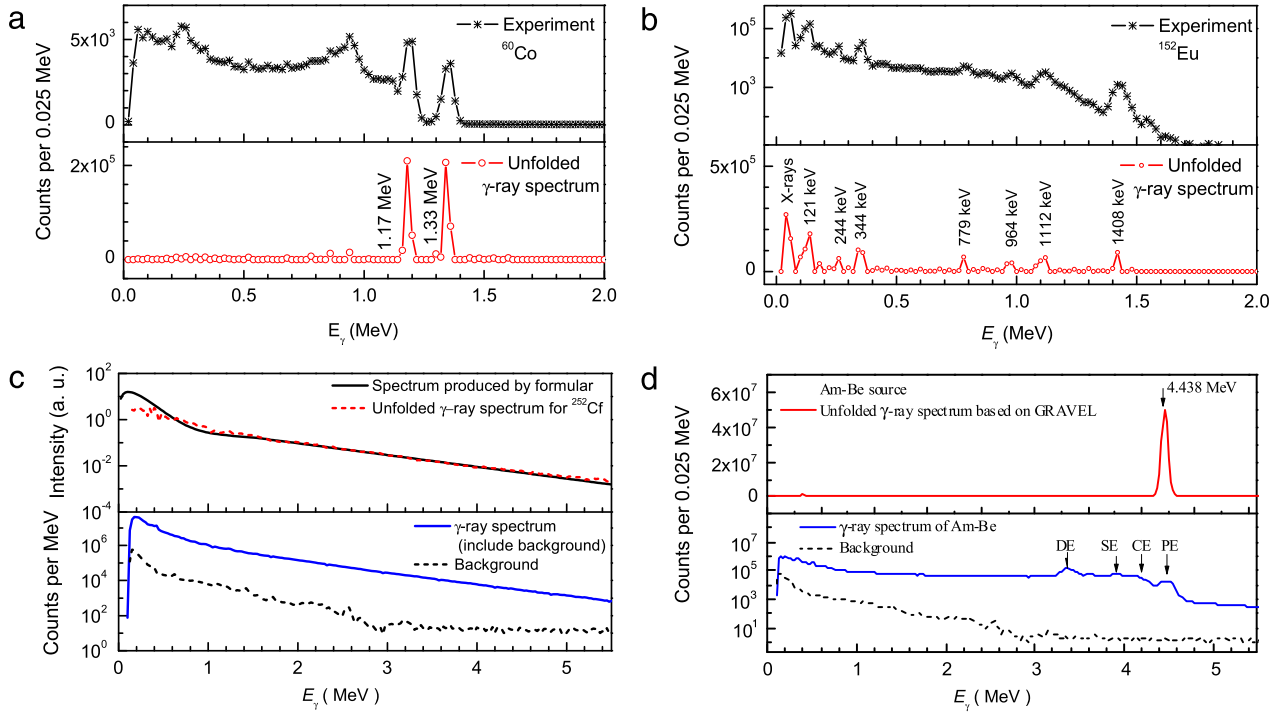

Fig. 11. The γ-ray spectra measured using the CLYC detector and real γ-ray spectra unfolded using the GRAVEL method: (a) ^{60}Co standard point source; (b) ^{152}Eu standard point source, (c) ^{252}Cf fission chamber, (d) neutron γ-ray mixed field from a ^{241}Am-Be source; the meaning of acronyms of DE, SE, CE and PE are as the same as shown in Fig. 9.

in Fig. 11(c) and (d), respectively. The unfolded γ-ray spectrum from the ^{252}Cf radioisotope agrees well with the spectrum generated by the formula (7) [28] in the energy region ranging from 0.4 to 5.5 MeV. The discrepancies below 0.4 MeV are attributed to the measuring energy threshold and the n/γ discrimination influence. The γ-ray spectrum for the Am-Be source is mainly the 4.438 MeV peak emitted from decay of the excited ^{12m}C resulting from the reaction ^{9}Be(α, n)^{12m}C, where an α particle is emitted from the ^{241}Am decay.

$$\frac{dN_\gamma}{dE} = \begin{cases} 375E^2e^{-E/0.109} + 0.468e^{-E/1.457} & E \le 1.5\ \text{MeV} \\ e^{-E/0.851} & E > 1.5\ \text{MeV} \end{cases} \quad (7)$$

The energy resolutions for 1.33 MeV and 4.438 MeV are 1.95% and 1.82%, respectively. These results are much better than those from liquid scintillators, such as BC501A and BC537 detectors [29]. It can be concluded that – compared to a liquid scintillator – the CLYC detector is the preferred detector for γ-ray measurement in mixed n/γ fields.

4. Conclusion

The CLYC scintillator detector used in this work exhibits excellent linearity and energy resolution for γ-ray radiation. The γ-ray response function and efficiency were simulated and validated using standard γ-ray sources and^{252}Cf neutron source.

Compared with the commonly used liquid scintillator BC501A, the results presented in this work indicate that CLYC detector has higher γ-ray efficiency, the better energy resolution and n/γ discrimination performance. The CLYC detector is not only suitable for neutron measurement, but also a preferred detector for accurate γ-ray spectra in the mixed n/γ fields.

Acknowledgments

The authors would like to thank the National Science Foundation of China (Grant No. 11575165) for their funding support in carrying out this work, and we also like to thank to Jiansheng Li at INPC of CAEP for providing the ^{252}Cf source.

References

[1] V. Borrel, B. Kandel, F. Albernhe, et al., Fast neutron-induced damage in INTEGRAL n-type HPGe detectors, Nucl. Instrum. Methods Phys. Res. A 430 (1999) 348–362.
[2] C.M. Combes, P. Dorenbos, C.W.E. van Eijk, et al., Optical and scintillation properties of pure Ce^{3+}-doped Cs_2LiYCl_6 and Li_3Ycl_6: Ce^{3+} crystals, J. Lumin. 82 (1999) 299–305.
[3] A. Bessiere, P. Dorenbos, C.W.E. van Eijk, et al., Luminescence and scintillation properties of for gamma and neutron detection, Nucl. Instrum. Methods Phys. Res. A 537 (2005) 242–246.
[4] E.V.D. van Loef, P. Dorenbos, W.W.E. van Eijk, et al., Scintillation and spectroscopy of the pure and Ce3+-doped elpasolites: Cs_2LiYX_6 (X=Cl; Br), J. Phys.: Condens. Matter 14 (2002) 8481–8496.
[5] A. Bessiere, P. Dorenbos, C.W.E. van Eijk, et al., New thermal neutron scintillators: Cs_2LiYCl_6:Ce and Cs_2LiYBr_6:Ce, IEEE Trans. Nucl. Sci. 51 (5) (2004) 2970–2972.
[6] L. Trefilova, V. Cherginets, A. Gektin, et al., The inertia properties of Cs_2LiYCl_6:Ce scintillation crystals, Radiat. Meas. 42 (2007) 572–575.
[7] A. Giaz, N. Blasi, C. Boiano, et al., Fast neutron measurements with ^{7}Li and ^{6}Li enriched CLYC scintillators, Nucl. Instrum. Methods Phys. Res. A 825 (2016) 51–61.
[8] J. Glodo, R. Hawrami, K.S. Shah, Development of Cs_2LiYCl_6 scintillator, J. Crystal Growth 379 (2013) 73–78.
[9] N. D'Olympia, P. Chowdhury, C.J. Lister, et al., Pulse-shape analysis of CLYC for thermal neutrons, fast neutrons and gamma-rays, Nucl. Instrum. Methods Phys. Res. A 714 (2013) 121–127.
[10] N. D'Olympia, P. Chowdhury, E.G. Jackson, C.J. Lister, Fast nertron response of ^{6}Li-depleted CLYC detectors up to 20 MeV, Nucl. Instrum. Methods Phys. Res. A 763 (2014) 433–441.
[11] M.B. Smith, T. Achtzehn, H.R. Andrews, Fast neutron measurements using Cs_2LiYCl_6:Ce scintillator, Nucl. Instrum. Methods Phys. Res. A 784 (2015) 162–167.
[12] D.W. Lee, L.C. Stonehill, A. Klimenko, J.R. Terry, et al., Pulse shape analysis of Cs_2LiYCl_6:Ce scintillator for neutron and gamma-ray discrimination, Nucl. Instrum. Methods Phys. Res. A 664 (2012) 1–5.
[13] A.P. Simpson, S. Jones, M.J. Clapham, et al., Performance characteristics of a high efficiency passive neutron assay system using alternative neutron detectors to Helium-3, in: IEEE Nuclear Science Symposium and Medical Imaging Conference, 2011, pp. 4853–4857.
[14] Richard T. Kouzes, Azaree T. Lintereur, Edward r. Siciliano, Progress in alternative neutron detection to address the helium-3 shortage, Nucl. Instrum. Methods Phys. Res. A 784 (2015) 172–175.
[15] www.rmdinc.com.
[16] P.A. Rodnyi, V.B. Mikhailik, G.B. Stryganyuk, et al., Luminescence properties of Ce-doped $Cs_2LiLaCl_6$ crystals, J. Lumin. 86 (2000) 161–166.
[17] M.B. Chadwick, M. Herman, P. Oblozinsky, et al., ENDF/B-VII.1 nuclear data for science and technology: cross sections, covariances, fission product yields and decay data, Nucl. Data Sheets 112 (2011) 2887–2996.
[18] A. Kozorezov, J.K. Wigmore, A. Owens, Picosecond dynamics of hot carriers and phonons and scintillator non-proportionality, J. Appl. Phys. 112 (053079) (2012) 053079–1–053079–12.
[19] Pieter Dorenbos, Light output and energy resolution of Ce^{3+} -doped scintillators, Nucl. Instrum. Methods Phys. Res. A 486 (2002) 208–213.
[20] Wahyu Setyawan, Romain M. Gaume, Robert S. Feigelson, Stefano Curtarolo, Comparative study of nonproportionality and electronic band structures features in scintillator materials, IEEE Trans. Nucl. Sci. 56 (5) (2009) 2989–2996.
[21] Ivan V. Khodyuk, Pieter Dorenbos, Trends and patterns of scintillator nonproportionality, IEEE Trans. Nucl. Sci. 6 (59) (2012) 3320–3331.
[22] X-5 Monte Carlo Team, MCNP-A General Monte Carlo N-Particle Transport Code, Version 5. Vol. II: User's Guide.
[23] Jarek Glodo, William M. Higgins, Edgar V.D. van Loef, et al., Scintillation properties of 1 Inch Cs_2LiYCl_6:Ce crystals, IEEE Trans. Nucl. Sci. 55 (3) (2008) 1206–1209.
[24] M. Nakhostin, P.M. Walker, Application of digital zero-crossing technique for neutron-gamma discrimination in liquid organic scintillation detectors, Nucl. Instrum. Methods Phys. Res. A 621 (2010) 498–501.
[25] L.S. Birks, Handbook of X-ray Spectroscopy, Vol. I, CRC Press, Boca Raton, 1970, pp. 1–254.
[26] R. Machrafi, N. Khan, A. Miller, Response functions of Cs_2LiYCl_6:Ce scintillator to neutron and gamma radiation, Radiat. Meas. 70 (2014) 5–10.
[27] Marcel Reginatto, The "Multi-Channel" Unfolding Programs in the UMG Package: MXD_MC32 and IQU_MC32, and GRV_MC32 (Version 3.2). PTB, Germany, 2003.
[28] M. Palomba, G. D'Erasmo, A. Pantaleo, The monte Carlo code CSSE for the simulation of realistic thermal neutron sensor devices for humanitarian demining, Nucl. Instrum. Methods Phys. Res. A 498 (2003) 384–396.
[29] J.G. Qin, C.F. Lai, B.J. Ye, et al., Characterizations of BC501A and BC537 liquid scintillator detectors, Appl. Radiat. Isot. 104 (2015) 15–24.